Int J Earth Sci (Geol Rundsch) (2016) 105:1621–1636
DOI 10.1007/s00531-016-1305-4

ORIGINAL PAPER

# From folding to transpressional faulting: the Cenozoic Fusha structural belt in front of the Western Kunlun Orogen, northwestern Tibetan Plateau

**Cong Wang[1,2] · Xiao-Gan Cheng[1,2] · Han-Lin Chen[1,2] · Kang Li[1,2] · Xiao-Gen Fan[1,2] · Chun-Yang Wang[1,2]**

Received: 7 July 2015 / Accepted: 7 February 2016 / Published online: 2 March 2016


**Abstract** Fusha structural belt (FSB) is one of the most important tectonic units in front of the Western Kunlun Orogen, northwestern Tibetan Plateau (NW China), in which the Kekeya oil field was discovered in 1971. However, there is no new oil field discovered since then due to the unclarity of the intense and complex Cenozoic deformation in this area. Based on field investigation, seismic interpretation and Continuous Electromagnetic Profile data, we analyze in detail the Cenozoic deformation history, emphasizing on the spatial and temporal variation of the deformation of the FSB in this paper. The result suggests that the FSB was dominated by two deformation events, (1) early (Miocene–early Pliocene) folding event expressed by anticline, with the western segment E–W orienting, while the eastern segment NWW–SEE orienting and (2) later (since late Pliocene) transpressional faulting event that destroyed and divided the earlier anticline into a number of fault blocks. The transpressional faulting caused dextral strike-slip reverse fault, with the dip angles decreasing eastward from ~90° to <45°. The dextral strike-slip reverse fault developed in the core of the anticline in the western part which caused the anticline into several fault blocks, while in the eastern part, the fault developed in the north limb of the anticline with the core of the anticline reserved. Based on the spatial variation of structural characteristics, we propose that the fault block traps and anticline traps in the eastern segment and fault block traps in western segment are favorable for hydrocarbon accumulation.

**Keywords** Western Kunlun Orogen · Fusha structural belt · Folding · Transpressional faulting

## Introduction

The Western Kunlun Orogen is located in northwestern margin of the Tibetan Plateau, with a length of >1000 km and a width of ~100 km. Owing to the loading of overthrusting Western Kunlun in NW Tibetan Plateau, the Cenozoic foreland basin deposits accumulated along the southern Tarim block (Matte et al. 1996). A series of outcrops of the Cenozoic sequences in the piedmont provide a key for understanding the Cenozoic deformation history of northwestern Tibetan Plateau (Li et al. 1996; Wan and Wang 2002; Wang et al. 2003; Liu et al. 2004; Jiang et al. 2013). Moreover, as an important aspect of the foreland basin, the fold-and-thrust belt has great potential for hydrocarbon exploration, with the Kekeya oil field being discovered in the region at 1971 (Fig. 1). However, more recent oil field was not discovered since then until an exploring breakthrough in KD 1 well at the first row structure of the fold-and-thrust belt (Fusha structural belt, FSB) in 2010 (Figs. 1, 2). The success of the KD 1 well shows that FSB should have good prospective for future exploration. Unfortunately, the failure of some later wells (e.g., KD 101 well and KD 2 well) in FSB indicates the hydrocarbon accumulation of this region is more complex, due possibly to the unclarity of the intense and complex Cenozoic deformation process.

Due to the thick Quaternary loess at surface and steep structures at the FSB (Figs. 1, 2), the seismic data in this

✉ Xiao-Gan Cheng
chengxg@zju.edu.cn

[1] School of Earth Sciences, Zhejiang University, Hangzhou 310027, China

[2] Research Center for Structures in Oil and Gas Basin, Ministry of Education, Hangzhou, China

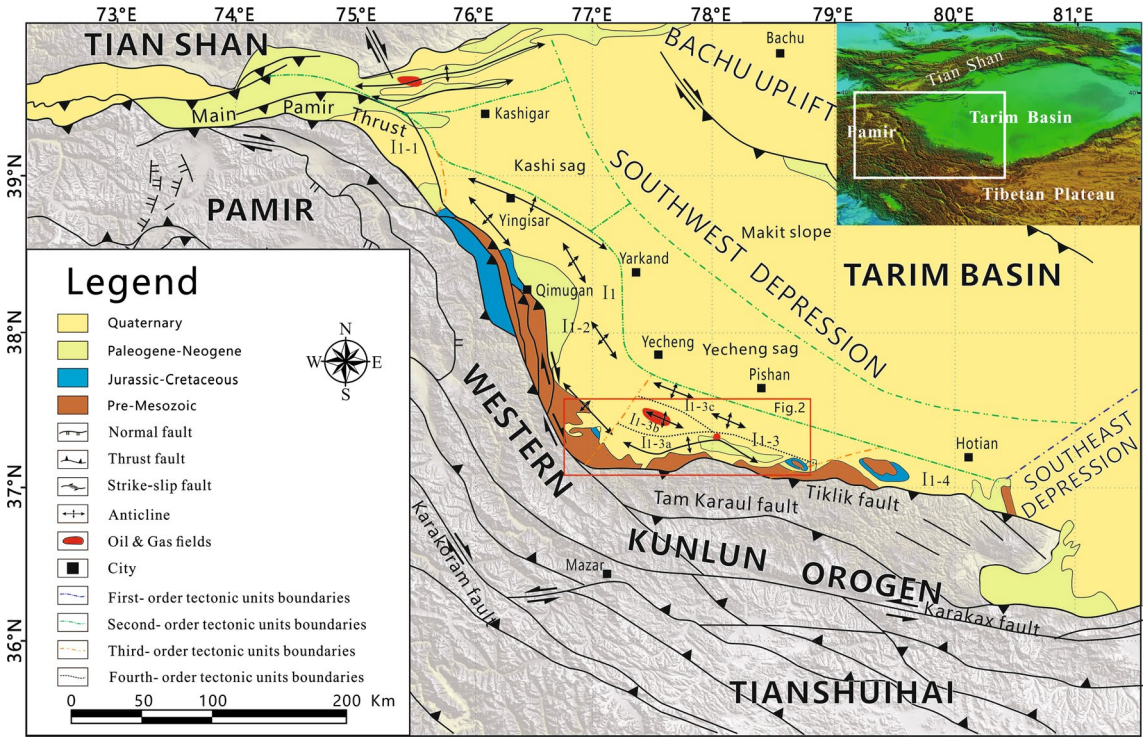


**Fig. 1** A simplified geological map of the southwest Tarim Basin and adjacent Tibetan Plateau, showing major Cenozoic faults and well-exposed Cenozoic deposits, based on Cowgill et al. (2003), Cowgill (2010), Cheng et al. (2012a, b), Robinson et al. (2012) and Cao et al. (2013). *I1* thrust belt in the front of the Western Kunlun Orogen, *I1-1* Wupor segment, *I1-2* Sugaite segment, *I1-3* Kedong segment, *I1-4* Hetian segment, *I1-3a* Fusha structural belt, *I1-3b* Kekeya structural belt, *I1-3c* Guman–Heshitake structural belt. The *red box* is the range of the study area

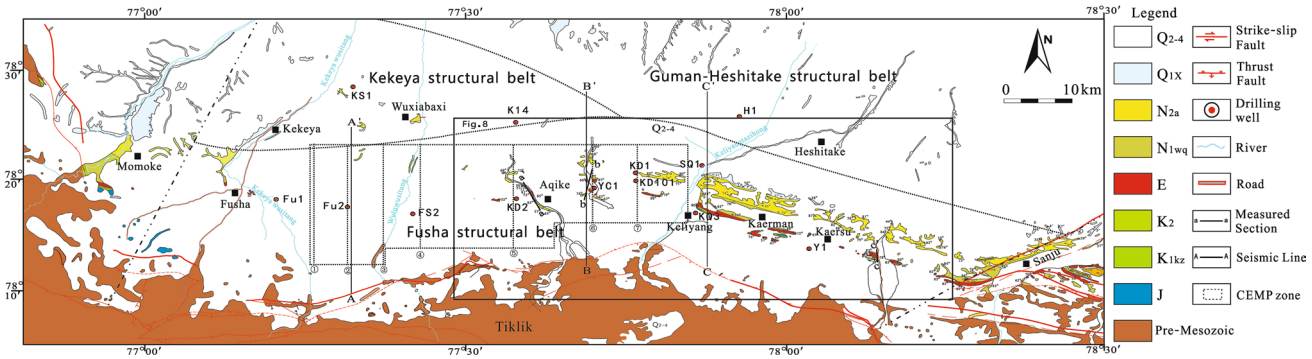


**Fig. 2** Regional geological map in Kedong area. $Q_{2-4}$ Quaternary alluvial and eolian sediments, $Q_{1x}$ Quaternary Xiyu Formation, $N_{2a}$ late Pliocene Artux Formation, $N_{1wq}$ Oligocene–Miocene Wuqia Group, *E* Eocene strata, $K_2$ Cretaceous Yingjisha Group, $K_{1Kz}$ Cretaceous Kezilesu Formation, *J* Jurassic sediments. The *dashed box* is the range of the CEMP zone. The original data are based on Institute of Petroleum Exploration and Exploitation, Tarim Oilfield Company, PetroChina

area are of low quality, resulting in ambiguity in structural model that hinders the hydrocarbon exploration. For example, some scientists considered the structural characteristics of the FSB are a typical triangle wedge style (Wu et al. 2004; Xiang 2006; Hu et al. 2008; Cheng et al. 2011). But Yang et al. (2011) suggested that the FSB was characterized by basement-involved structure at the back while by detachment structure in the front. Du et al. (2013) interpreted the FSB as a transpressional structure which consisted of steep basement fault and gently dipping backlimb and intensely deformed forelimb. However, the new 3D seismic data suggest that the vertical superposition seismic reflections do not exist (Du et al. 2013). The borehole data from the KD 101 well and KD 1 well indicate that the

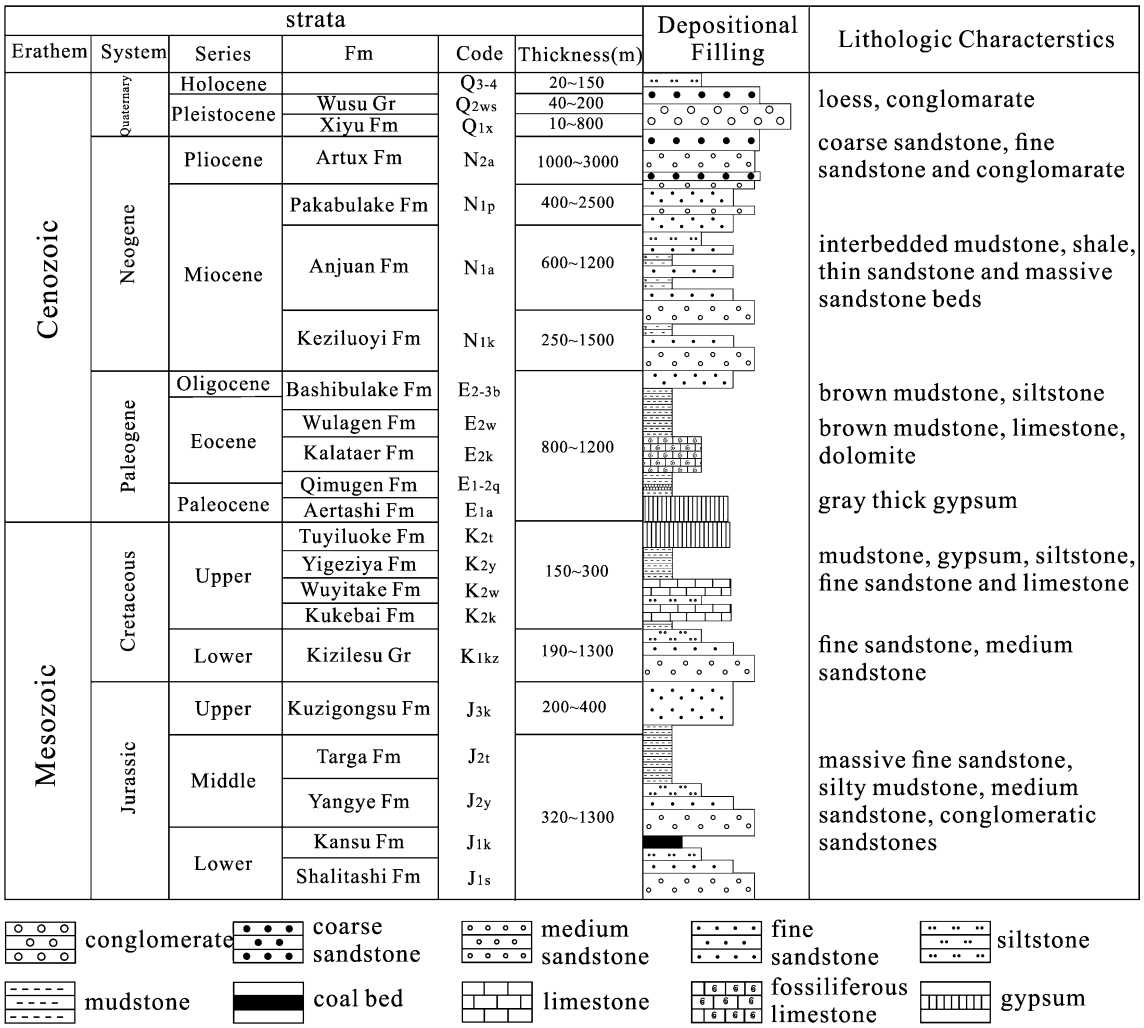


**Fig. 3** Jurassic to Quaternary stratigraphy in the front of the Western Kunlun Orogen

Cenozoic–Mesozoic sequences are not repeated, which is inconsistent with imbricated structure model interpreted by previous researchers (Wu et al. 2004; Xiang 2006; Cheng et al. 2011).

In order to get a relatively complete understanding of the Cenozoic evolution of the FSB, this paper analyzes the Cenozoic deformation architecture and deformation history of the FSB based on field geological investigation and 2D and recent 3D seismic and Continuous Electromagnetic Profile (CEMP) data (Fig. 2).

## Geological setting

The Cenozoic collision and long-lasting convergence between Indian plate and Eurasian plate have resulted in regional deformation in Central Asia since ca. 55 Ma (Patriat and Achache 1984; Searle et al. 1987; Clift et al. 2002; DeCelles et al. 2002), resulting in rejuvenation of many paleo-orogens, i.e., Tian Shan, Kunlun Shan and Qilian Shan, and major boundary faults, i.e., Karakorum and Altyn Tagh faults (Tapponnier et al. 1986). The rapid uplift and northward thrusting of the Western Kunlun Orogen (Sobel and Dumitru 1997; Arnaud et al. 2003; Wang et al. 2003), as well as rapid northward penetration of the Pamir syntax (Sobel and Dumitru 1997; Burtman 2000; Robinson et al. 2004, 2007; Bershaw et al. 2012), led to development of Cenozoic Southwest Tarim foreland basin.

The Southwest Tarim foreland basin can be divided into four tectonic units, i.e., the thrust belt in front of Western Kunlun Orogen, Yecheng–Kashi depression, Markit slope and Bachu–Tazhong forebulge (Fig. 1). The thrust belt can be further subdivided into Wupor, Sugaite, Qimugen, Kedong and Hetian segments from northwest to southeast (Cheng et al. 2012a, b). The FSB is one of the southernmost row structures of Kedong segment and exhibits a

northward convex shape, with ~210 km length and ~30–50 km width (Fig. 1).

In front of Western Kunlun Orogen, the Mesozoic–Cenozoic stratigraphy consists of continuous sequences (Fig. 3) (Jin et al. 2003; Zhang et al. 2003; Jia 2004). The Lower Jurassic strata are characterized by massive fine-grained sandstone and silty mudstone with coal beds, which have been interpreted as fan-delta facies (Zhang et al. 2000). The Middle Jurassic strata include Targa and Yangye Formations, which are dominated by laterally continuous gray siltstone, tabular sandstone and organic-rich shale representing overbank and lacustrine deposition (Sobel 1999; Zhang et al. 2000). The Upper Jurassic Kuzigongsu Formation comprises gray fine-grained sandstone, siltstone and conglomerates interpreted as deposition of braid delta and alluvial plain facies (Sobel 1999; Zhang et al. 2000; Fang et al. 2009). The Lower Cretaceous Kezilesu Group comprises packages of dark-red clastic rocks and varies in thickness between 190 and 1300 m, with the main depocenter located in Qimugan region (Cheng et al. 2012a). The upper Cretaceous Yengisar Group include Kukebai, Wuyitake, Yigeziya and Tuyiluoke Formations, composed of clastic rocks, gray limestone and red gypseous mudstone of marine facies (Zhang et al. 2003; Cheng et al. 2012a), with a total thickness between 150 and 300 m (Fig. 3). A series of marine carbonate rocks and gypsum layers deposited during the late Cretaceous to Eocene forms important cap rocks in Southwest Tarim foreland basin (Xing et al. 2012; He et al. 2013), with thickness varying from 150 to 1200 m (Fig. 3). The late Cenozoic sequences are dominated by non-marine sediments, which consist of reddish sandstone, gray-green siltstone and conglomerate (Jin et al. 2003), with a total thickness about 4000 m.

## The geometry of FSB

In this paper, we obtain one prestack time-migrated 2D seismic line ($A$–$A'$) and two prestack time-migrated 3D seismic lines ($B$–$B'$ and $C$–$C'$) to decipher the geometry of the FSB (Fig. 2). The prestack time-migrated 2D and 3D seismic lines were carried out in 2011 by CNPC (China National Petroleum Corporation). The collection, stacking and processing methods are unknown. These prestack time-migrated lines were converted to depth seismic sections using velocities for each stratigraphic unit constrained by Vertical Seismic Profiling (VSP) data from the drilling well KD 101 using the MOVE software (Midland Valley, Glasgow, UK). Also, the logging data were used to define seismic facies and conduct stratigraphic correlations in these seismic profiles.

Seismic profile $A$–$A'$ is located in Wuxiabaxi area near to Fu2 well, with an orientation of profile substantially perpendicular to structural striking of FSB (Fig. 2). Based on the geological outcrop and seismic reflection, this section is characterized by a syncline in the north and an anticline in the central part (Fig. 4). Through the detail interpretation of the architecture inner the anticline, a high-angle thrust fault (F3) and its branch faults have been identified which possibly consist of positive flower structure. In the southern part of the profile, the Upper Paleozoic thrusted onto the Quaternary along a high-angle thrust fault (F1) (Fig. 4).

Seismic profile $B$–$B'$ is located in the middle part of FSB, adjacent to Yuliqun area, with a orientation substantially perpendicular to the tectonic line of FSB (Fig. 2). The Paleogene sequences show a clear strong continuous reflection in both south and north segments (Fig. 5), while the central segment is dominated by a chaotic reflection. The range of this chaotic reflection zone is consistent with the steep dipping strata controlled by two steep faults cropped out on the surface. Based on the geological outcrop and seismic reflection, this section is characterized by an anticline which was cut by steep faults (Fig. 5). The growth strata developed in the north limb of the anticline indicate that the folding of the FSB began at the early Pliocene.

Seismic profile $C$–$C'$, approximately perpendicular to structural striking, is situated on the eastern segment of FSB, adjacent to Keliyang area (Fig. 2). Both outcropped northern and southern segments are composed of the Quaternary sediments, while continuous strata spanning the Jurassic to Quaternary from south to north with nearly vertical dip angles are preserved in the central segment. The refection is clear and continuous in both southern and northern segments (Fig. 6), similar to that in $A$–$A'$ and $B$–$B'$ profiles. An anticline exhibits in the southern segment, while the northern segment expresses monocline reflections. A steeply south-dipping fault (F3) and a north-dipping and another south-dipping branch thrust faults can be identified in the central segment of the profile. The attitudes in central segment are approximately vertical, and some of pre-Mesozoic strata are uplifted onto the surface. However, the attitudes decreased gradually in the northern segment of the profile. Compared with steep faults in $A$–$A'$ and $B$–$B'$ profiles, the fault (F3) plane of the $C$–$C'$ profile begins to manifest south dipping.

## Determination of property for the high-angle fault (F3) in the FSB

### Characteristics of CEMP section in the FSB

The CEMP data, covering an area of c. 800 km$^2$ with line density of 500 m × 500 m in the piedmont of the Western Kunlun Orogen (Fig. 2), were carried out in 2011 by

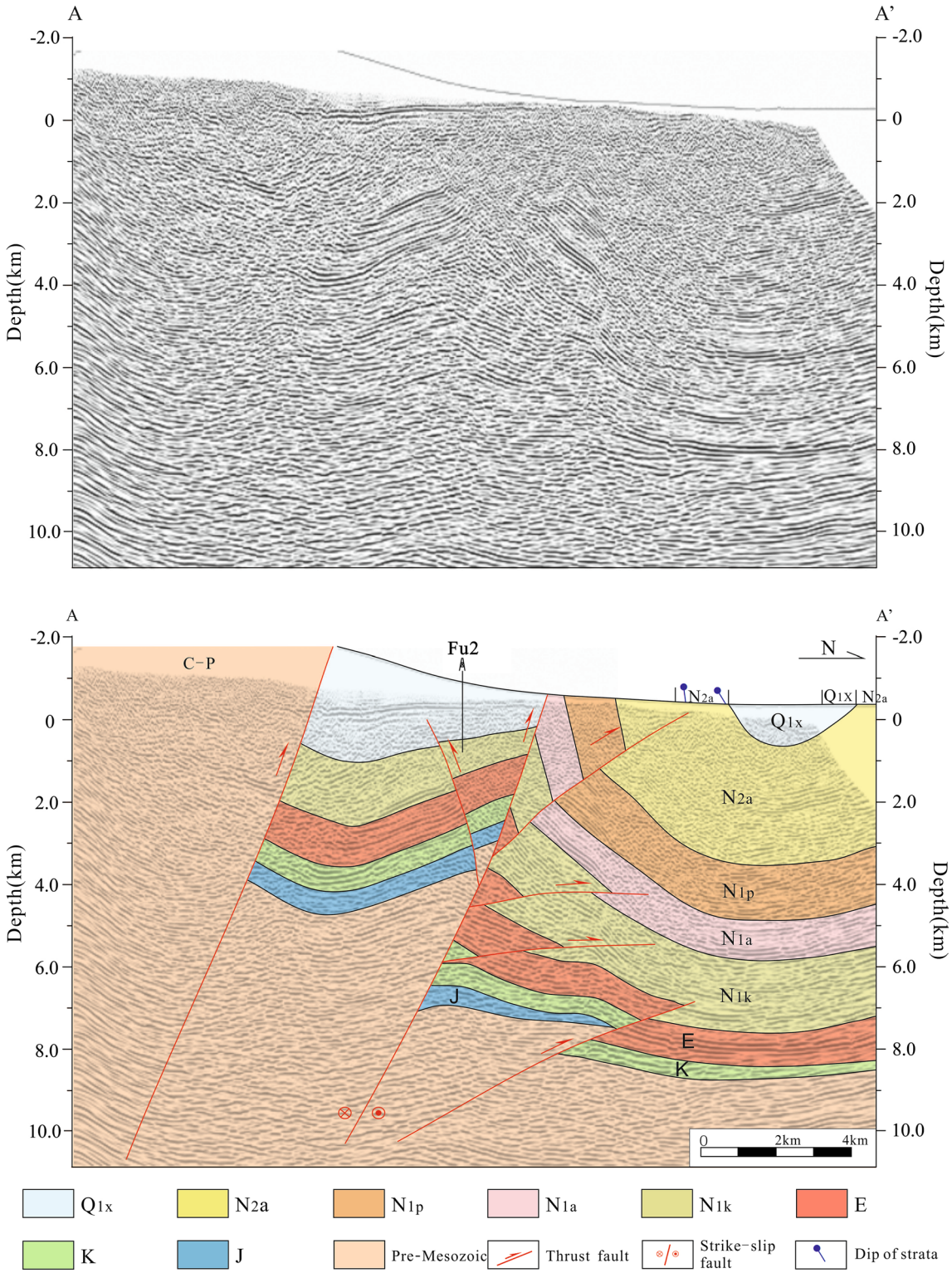


**Fig. 4** Geological interpretation of *A–A′* seismic profile in FSB. $Q_{1x}$ Quaternary Xiyu Formation, $N_{2a}$ late Pliocene Artux Formation, $N_{1p}$ Miocene Pakabulake Formation, $N_{1a}$ Miocene Anjuan Formation, $N_{1k}$ Oligocene–Miocene Keziluoyi Formation, *E* Eocene Kashi Group, *K* Cretaceous sediments, *J* Jurassic sediments. The *blue dots* and *oblique lines* represent the strata dips of the outcrop section

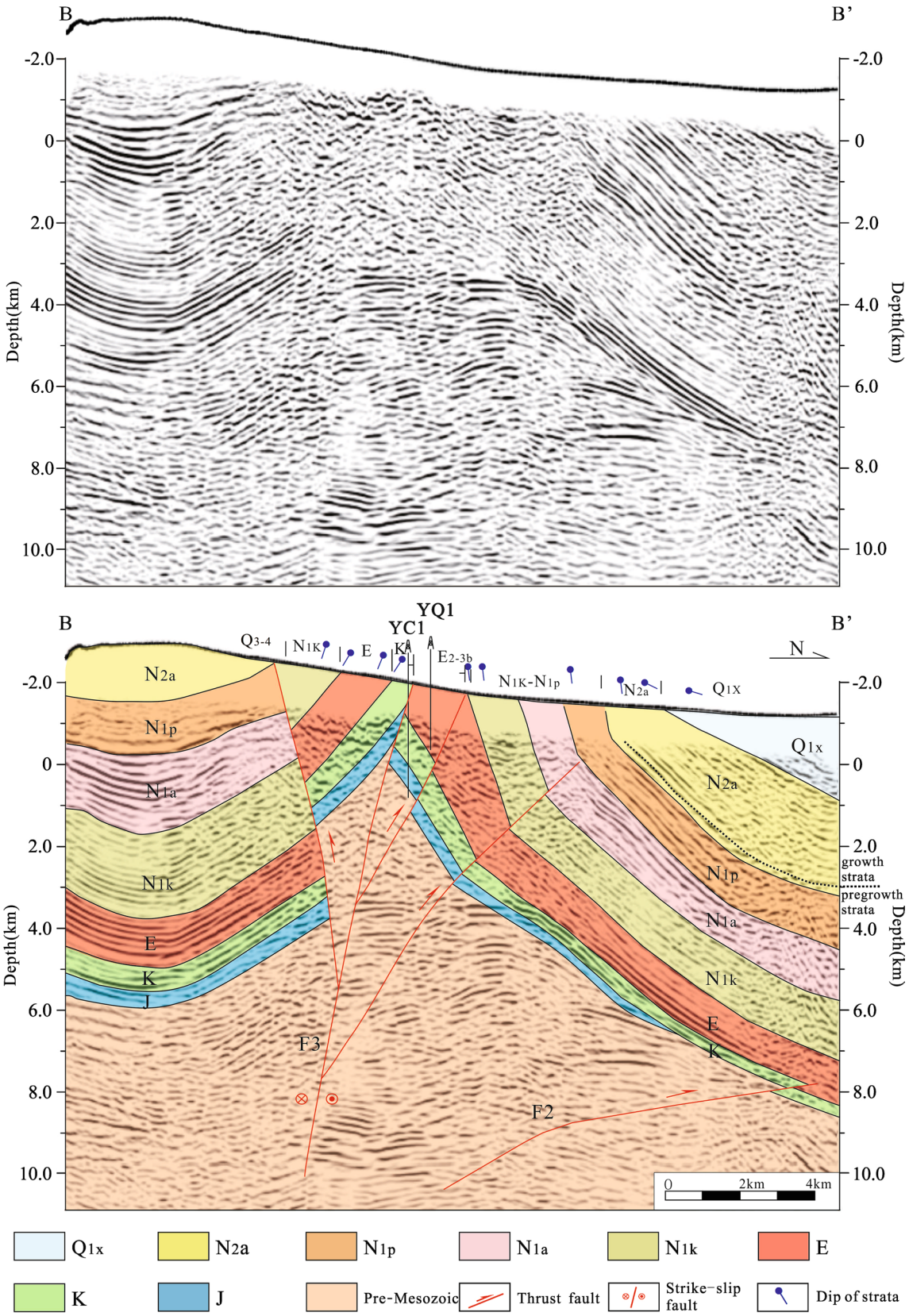


**Fig. 5** Geological interpretation of *B–B′* seismic profile in FSB. $Q_{1x}$ Quaternary Xiyu Formation, $N_{2a}$ late Pliocene Artux Formation, $N_{1p}$ Miocene Pakabulake Formation, $N_{1a}$ Miocene Anjuan Formation, $N_{1k}$ Oligocene–Miocene Keziluoyi Formation, *E* Eocene Kashi Group, *K* Cretaceous sediments, *J* Jurassic sediments. The *blue dots* and *oblique lines* represent the strata dips of the outcrop section

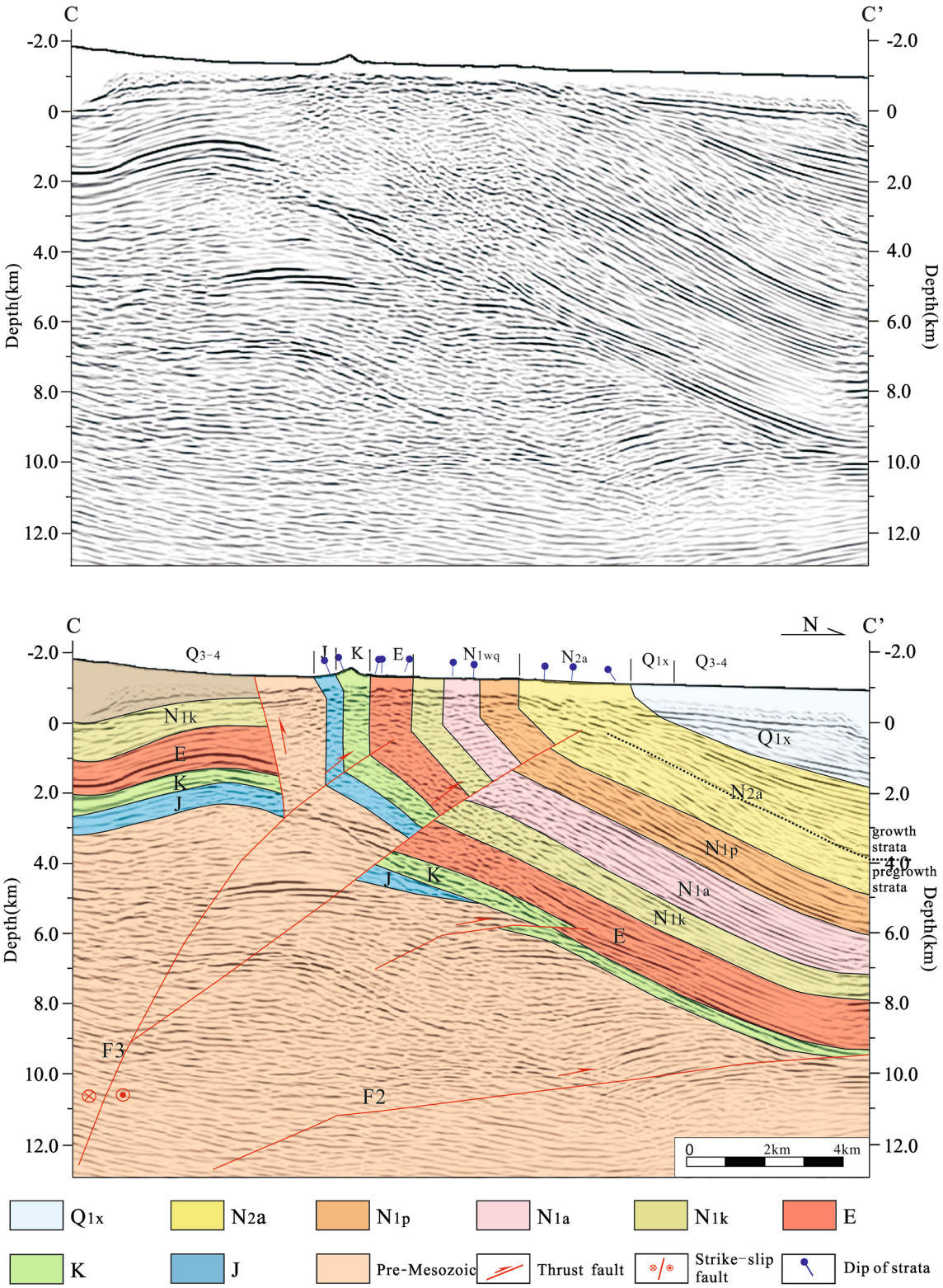


**Fig. 6** Geological interpretation of *C–C′* seismic profile in FSB. $Q_{1x}$ Quaternary Xiyu Formation, $N_{2a}$ late Pliocene Artux Formation, $N_{1p}$ Miocene Pakabulake Formation, $N_{1a}$ Miocene Anjuan Formation, $N_{1k}$ Oligocene–Miocene Keziluoyi Formation, *E* Eocene Kashi Group, *K* Cretaceous sediments, *J* Jurassic sediments. The *blue dots* and *oblique lines* represent the strata dips of the outcrop section

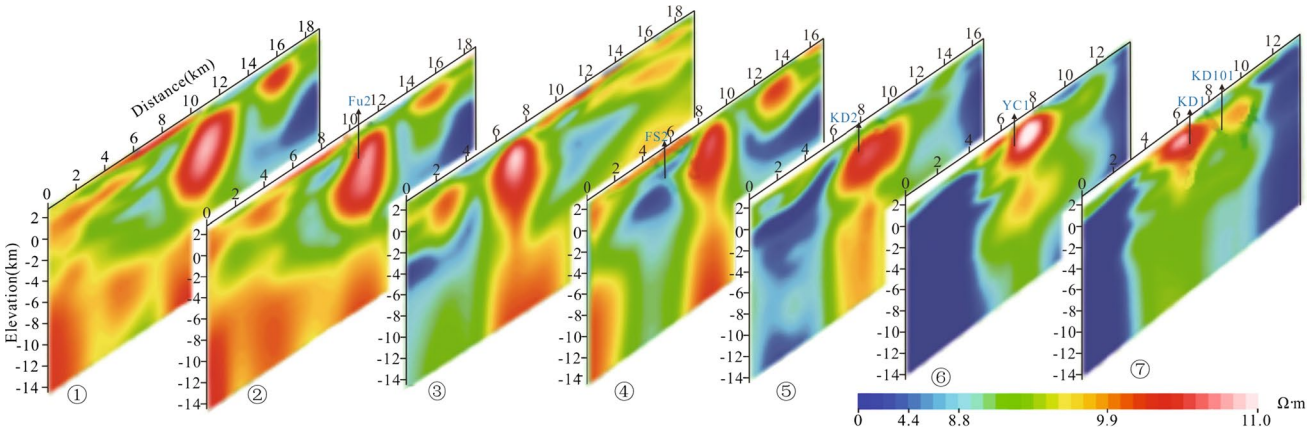


**Fig. 7** CEMP section in Fusha structural belt (the original data are based on Institute of Petroleum Exploration and Exploitation, Tarim Oilfield Company, PetroChina)

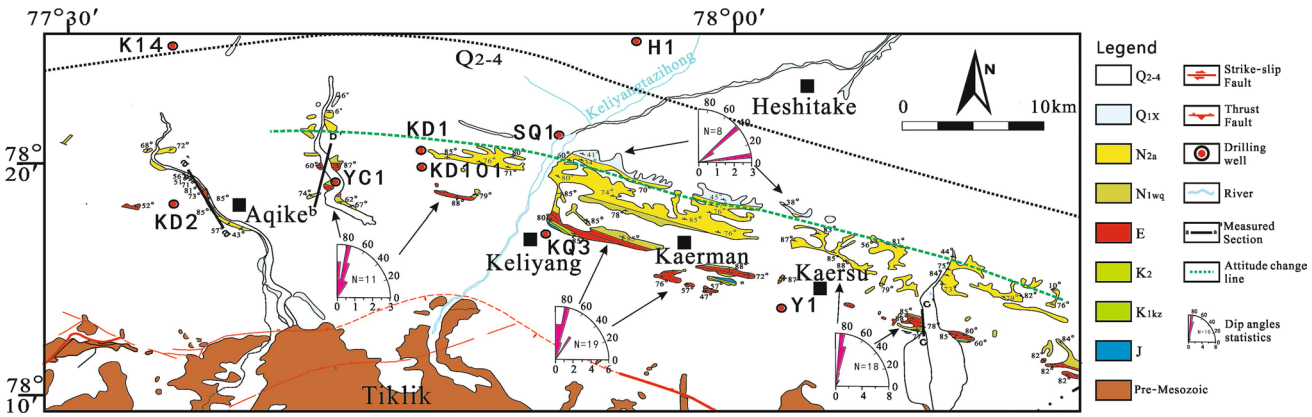


**Fig. 8** The distribution of dip angle and measuring outcrop sections in FSB. $Q_{2-4}$ Quaternary alluvial sediments, diluvial sediments and eolian sediments, $Q_{1x}$ Quaternary Xiyu Formation, $N_{2a}$ late Pliocene Artux Formation, $N_{1wq}$ Oligocene–Miocene Wuqia Group, $E$ Eocene strata, $K_2$ Cretaceous Yingjisha Group, $K_{1Kz}$ Cretaceous Kezilesu Formation, $J$ Jurassic sediments

CNPC. Unknown processing procedures of original data were carried by CNPC.

The correlations between the stratigraphic and electrical units have been established, with (1) low resistive layer corresponding to the Neogene sequences; (2) second high resistive layer corresponding to the Mesozoic sequences; (3) first high resistive layer corresponding to the Paleozoic–Proterozoic and Quaternary (Chen et al. 2010). The CEMP section in FSB is characterized by zonal features from south to north (Fig. 7). The uppermost parts in the south and north of the sections are featured by high resistance, corresponding to the Quaternary. The deep parts in the south and north of the sections are characterized by the second high resistive layer and first high resistive layer, corresponding to the Paleogene–Mesozoic and Paleozoic–Proterozoic, respectively. The central parts of the sections are dominated by the high resistive layer with triangle shapes, which are continuously stable from the east part of FSB to FS 2 well. The borehole data from the YC 1, KD 1 and KD 101 wells suggest that this continuously stable high resistive layer is consistent with steeply dipping Cretaceous–Eocene strata cut by several faults (Zeng et al. 2011). The first high resistive layer in the central part extends to the deep, reaching 14,000 m or deeper, which suggests that the exposed steeply dipping Cretaceous–Eocene strata were not likely to be thrusted directly by the southern thrust fault as previously interpreted (Qu et al. 1998, 2005; Xiao et al. 2000; Liu et al. 2004; Wu et al. 2004). A possible interpretation is that these steeply dipping Cretaceous–Eocene strata were thrusted to surface by strike-slip reverse faults.

## The attitude change of outcrops in the FSB

For the FSB, most part is covered by the Quaternary strata, and a series of Mesozoic–Cenozoic strata are exposed only in Aqike, Keliyang, Kaersu and Sulaazi areas (Figs. 2, 8).

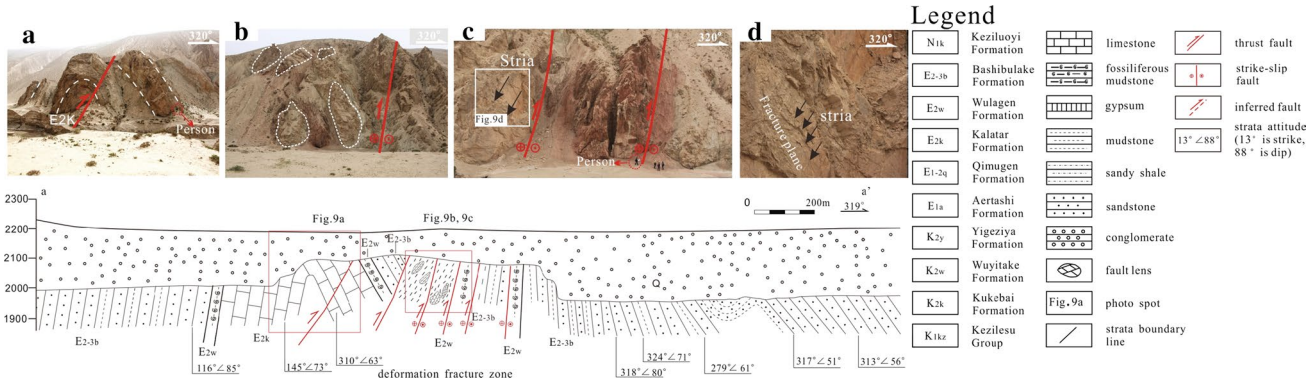


**Fig. 9** Geological section in Aqike area

The dip angles of these strata are steep, and some are more than 70°. The range of the high-angle strata is consistent with the chaotic reflection in the seismic profiles and first high resistive layer in the CEMP section. Meanwhile, an attitude change zone, which trends to northwest, is identified at surface in the north part of the FSB. The dip angles are more than 70° in the southern portion, but decrease sharply to less than 50° in the northern portion (Fig. 8). This phenomenon is interpreted as that the FSB is controlled by the blind thrust faults, which is consistent with the interpretation in the seismic profiles (Figs. 4, 5, 6).

## The deformation characteristic of different outcrop sections in the FSB

### *Aqike section*

The Aqike section is located in the west of YC 1 well and is measured from the 37°18′27.77″N, 77°35′70.24″E to 37°18′01.17″N, 77°35′54.97″E (Figs. 8, 9). The strata outcropped in this section span the Eocene to Pliocene which consist of Kalatar, Wulagen, Bashibulake and Artux Formations. An anticline, with its core consisting of Kalatar Formation, develops in the middle part of this section. The Kalatar Formation in southern limb of the anticline strikes 145° and dips 73°, while strikes 310° and dips 63° in the northern limb (see photograph in Fig. 9a). The Eocene strata in the northern limb of the anticline are deformed by a set of steep NE-trending faults and form a c. 200-m-wide strong fracture zone (see photograph in Fig. 9b, c). This zone is characterized by tectonic lenses consisting of limestones of Kalatar Formation and calcareous breccia of Wulagen Formation, and mudstone matrixes from Bashibulake Formation are prevalent within the zone (Fig. 9b, c). These tectonic lenses, 1–3 m and up to 10 m in diameter in some places, indicate intense activity of faults (Fig. 9b). The dip angle of Wulagen and Bashibulake Formations exposed in the north of the deformation fracture zone is approximately vertical. The dip angle of Bashibulake Formation in northern segment of this section decreases to 53°. A set of north–northeast striking and steeply southeast-dipping faults with fault striae of low dip angles can be recognized in this zone (see photograph in Fig. 9d). Based on the brittle shear-sense indicators such as striae, steeply southeast-dipping faults were dextral strike-slip faults and the deformation fracture zone was a dextral strike-slip fracture zone (see photographs in Fig. 9b–d).

### *Yuliqun section*

Yuliqun section lies in west side of KD 1 well, adjacent to YC 1 well, and is measured from 37°17′30.01″N, 77°41′36.38″E to 37°19′26.44″N, 77°41′25.80″E (Figs. 8, 10). The exposed sediments span from the Jurassic to Neogene strata. This section is featured by fault contact between Jurassic Yarkand Group and Paleo-Eocene Qimugen Formation, and a deformation fracture zone, with the Kalatar, Qimugen and Wulagen Formations involved, is identified between the Aertashi and Bashibulake Formations in the north. The fault contact between Yarkand Group and Qimugen Formation implies that the fault is a reverse fault, and the opposite dipping between hanging wall and foot wall maybe implies that a anticline was cut by this fault and the hanging wall and foot wall represent two limbs of anticline. In the fracture zone, series of thrust faults are found in this fracture zone. Some tectonic lenses are observed in the internal fracture zone, with a maximum diameter up to c. 1 m (see photograph in Fig. 10c), suggesting an intense fault activity. The interbed shear fabrics (see photograph in Fig. 10a) indicate a nature of dextral strike-slip reverse fault.

### *Sulaazi section*

Sulaazi section lies in the east of FSB and is adjacent to Keziyigele area (Figs. 8, 11). The sediments spanning

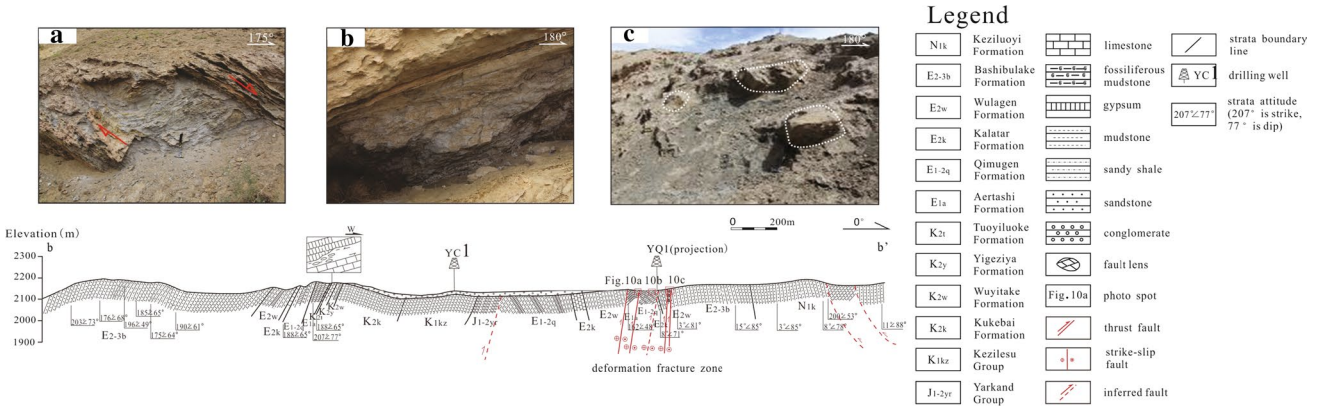


**Fig. 10** Geological section in Yuliqun area

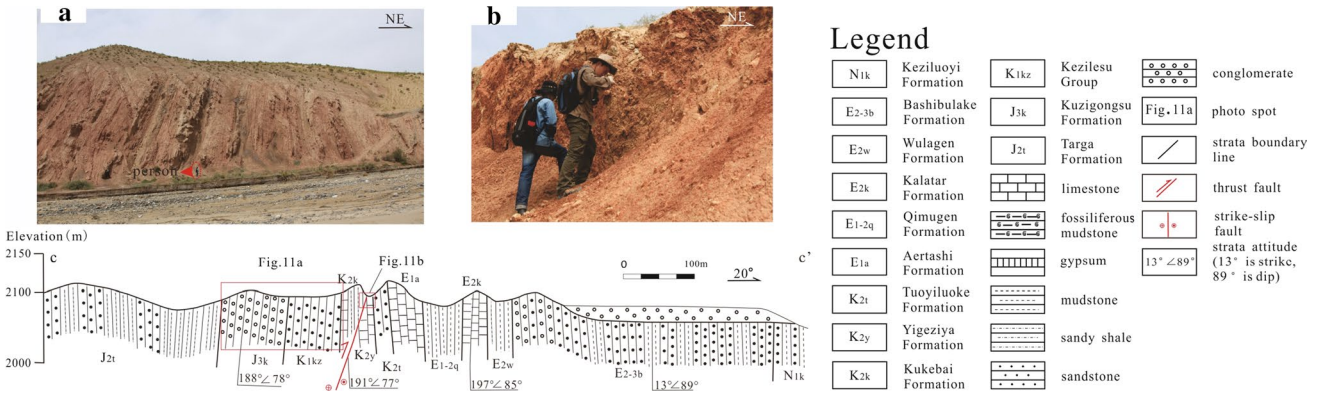


**Fig. 11** Geological section in Sulaazi area

from the Jurassic to Neogene strata are exposed along a riverbed near Sulaazi from south to north. These strata are now quite steep with dip angles up to >75° (see photographs in Fig. 11a, b). A 1- to 2-m-wide fracture zone which is controlled by a reverse fault is observed between the Kukebai and Yigeziya Formations in the middle part of the Sulaazi section. This fracture zone consists of severely broken limestone of Yigeziya Formation (see photograph in Fig. 11b). Compared with the Aqike and Yuliqun sections, the scale of the fracture zone in the Sulaazi section becomes significantly smaller, suggesting that the activity intensity of the fault becomes significantly weak. The features described in this section suggest that the fault in the Sulaazi section is the same as that in the Aqike and Yuliqun sections.

Based on the geological survey, CEMP data and 3D and 2D seismic profiles, the complex chaotic reflection zone developed in the FSB is interpreted to be a dextral strike-slip reverse fault zone. Moreover, the whole characteristic of the FSB is an anticline which is destroyed by later transpressional faulting (Fig. 12).

## The extending scale and activity of the strike-slip reverse fault

The strike-slip reserve fault zone is 200–300 m wide and consists of giant tectonic lens at the Aqike (see photographs in Fig. 9b, c) and Yuliqun sections (see photograph in Fig. 10c), indicating intense activity of the strike-slip reserve fault, while the phenomenon of the 1- to 2-m-wide strike-slip reserve fault zone and small tectonic breccias (see photograph in Fig. 11b) at the Sulaazi section suggests that the activity intensity of the strike-slip reserve fault decreases rapidly toward east.

In the western segment of the FSB, the features of the seismic profiles are dominated by positive flower structures, indicating that the strike-slip reverse fault has existed (see profiles ① ② ③ in Fig. 12). In the middle segment of the FSB, the dip angles of the strata in the south are small, while those in the central are almost vertical forming obvious positive flower structures. In the eastern segment of the FSB, the strike-slip reverse fault cuts through the north limb in the Keliyang section and extends eastwardly (see

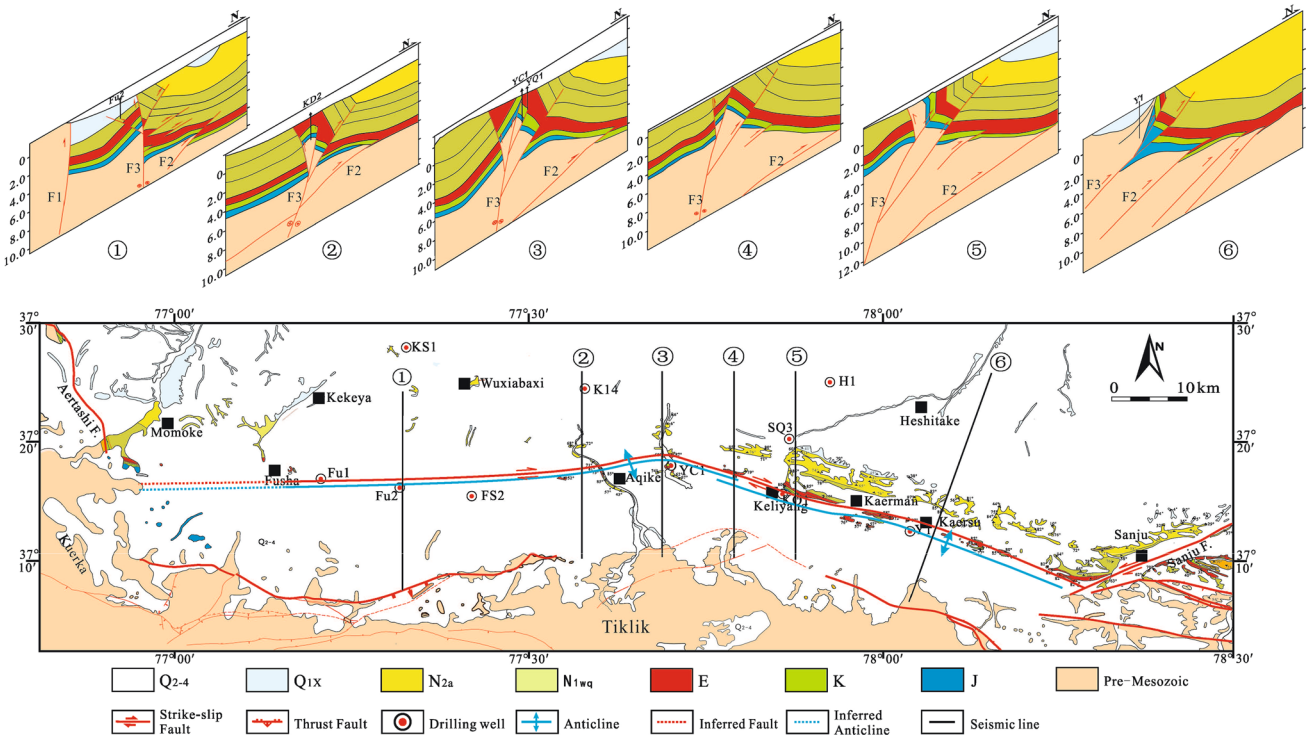


**Fig. 12** Spatial change of the structural style in the FSB

profiles ④ ⑤ in Fig. 12). In the easternmost of the FSB, the main structure indicates that the deformation is dominated by thrusting rather than strike-slipping. Therefore, the strike-slip reverse fault varies its expression spatially. It is speculated that the strike-slip reverse fault extends westward to the west of Yecheng area, and intersects the Aertashi fault, while it prolongs eastward to the east of Sanju area and may intersect the Sanju sinistral strike-slip fault (Zhang et al. 2011; Cheng et al. 2012b). In a planar view, the strike-slip reverse fault exhibits northward convex shape. The orientation changed from E–W direction along the western part to NW direction along the eastern part, and the dip angles decreased eastward from ~90° to <45°.

### Spatial overlay relations between strike-slip reverse fault (F3) and anticlines

Two anticlines are identified in the FSB in early stage and superpose in the Keliyang area through the geological survey and 2D and 3D seismic profiles (see profile ④ in Fig. 12). The western anticline distributes in E–W trend, while the eastern anticline shows NWW trend, parallel to the strike-slip reverse fault. The shape of the western anticline is tight, and the Eocene strata are exposed in the core of the anticline in Aqike area, and the Cretaceous strata are exposed in the core of the anticline in Yuliqun area. In contrast, the eastern anticline is a broad fold, and the core of the anticline is exposed by the Jurassic strata in Kaersu area.

## Discussion

### Deformation time of the FSB

The growth strata, which recorded the growth process of tectonic deformation, can be used to constrain the time of the tectonic deformation (Suppe et al. 1992). In the pediment of the Western Kunlun Orogen, obvious growth strata have been identified (Chen et al. 2001). The growth strata, which is identified in the seismic profiles (Fig. 5), initiated in the bottom of the Artux Formation, indicating that the Fusha anticline developed in the Artux Formation deposition. Combined with the surrounding magnetostratigraphic data (Sun and Liu 2006), the Fusha anticline developed in the early Pliocene.

An unconformity between the Wusu Group and the Paleo-Neogene Formations from the geological survey indicates that a regional tectonic movement initiated after the deposition of Xiyu Formation. In addition, the later dextral strike-slip reverse fault was truncated and overlain by the approximately horizontal Wusu Group (Fig. 9), which suggests that the fault initiated before the deposition of Wusu Formation. The magnetostratigraphic data and

geological survey from the Kekeya section show the Xiyu Formation initiated at ~3.5 Ma (Zheng et al. 2000) and terminated at ~1.3 Ma (Chen et al. 2001). Therefore, we propose that the later dextral strike-slip reverse fault may initiated in the late Pliocene, while the exact time still needs more study in the future.

## Cenozoic tectonic evolution of the FSB

The FSB belonged to the northern part of the Paratethys in Paleogene (Dercourt et al. 1993) and experienced multiple-stage regression and transgression processes (Yin et al. 2002; Bosboom et al. 2011; Sun and Jiang 2013), which resulted in forming a series of marine carbonate rocks, clastic rocks and mudstone (Sobel 1999; Zhang et al. 2000; Jin et al. 2003; Jia 2004; Wang et al. 2014). In Miocene, due to the continuous intracontinental strain resulting from the collision between Indian and Eurasian plates, Pamir syntax moved rapidly northward (Sobel and Dumitru 1997; Burtman 2000; Coutand et al. 2002; Robinson et al. 2004, 2007; Bershaw et al. 2012), and the Kashgar–Yecheng transfer fault system initiated (Cowgill 2010). The Keziluoyi, Anjuan and Pakabulake Formations were deposited during this time, with sediment sourced from the Western Kunlun Orogen based on the sandstone composition (Zheng et al. 2002, 2006). But the relief of the Western Kunlun Orogen was lower than present, and the tectonic activity was weak (Zheng et al. 2000, 2003a, b). In early Pliocene, with the rapidly northward convergence of the Indian plate, the uplift of the northwestern margin of the Tibetan Plateau was commenced, and Tiklik terrane started to thrust northward (Zheng et al. 2000; Jin et al. 2003; Wang et al. 2003; Li et al. 2007), resulting in fault-propagation fold forming in the FSB (Liu et al. 2004; Wu et al. 2004; Cheng et al. 2011). From middle Pliocene to early Pleistocene, the Pamir syntax underwent northward thrusting and tectonic rotation (Sobel and Dumitru 1997; Burtman 2000; Robinson et al. 2004, 2007; Bershaw et al. 2012), while the Western Kunlun Orogen experienced significantly accelerated uplift process (Zheng et al. 2006; Li et al. 2007; Liu et al. 2010), and the Tiklik terrane showed significantly northward convergence. The northeast oblique compressive stress resulted in transpressional faulting, which split the complete anticline forming in early Pliocene into several fault blocks in the FSB. Although the Tiklik terrane continued to uplift, the rate and northward compressive stress decreased significantly, and loose conglomerate and loess deposited in the FSB since late Pleistocene (Jin et al. 2003; Zheng et al. 2006; Si et al. 2007). Therefore, the FSB has undergone two phases of tectonic superposition since Miocene. The first stage is contraction deformation that caused the fault-propagation fold with complete anticlines in the FSB. The second stage is dominated by transpressional deformation that developed the steeply dipping strike-slip reverse fault which destroyed the complete anticlines. The second stage of transpressional sense of deformation suggests that the regional stress might change into compression with dextral strike-slip component in late Pliocene, which is consistent with the fact that the study area located between the sinistral Altyn Tagh fault and the dextral Kashgar–Yecheng transfer fault system. We speculate that the transpressional sense of deformation should be attributed to the impact of these two major strike-slip fault systems.

In addition, the tectonic evolution is diverse between west segment and east segment (Fig. 13). The lateral strike-slip reverse fault cuts through the anticline in different positions of the anticline. The north limb of the west anticline is cut through by lateral strike-slip reverse fault and shows as a monocline, while the deep part of the south segment of the west anticline retains the anticline shape. But the late strike-slip reverse fault cuts the east anticline at the north limb, and the core of anticline is reserved at the south, and there is an anticline shape on the surface. The rework of later transpressional deformation on previous anticlines in FSB implies that evolution of the fold-and-thrust belt in the Western Kunlun Orogen is more complex than a simple forward propagation model as previously thought.

## Hydrocarbon accumulation significance

There had been no breakthrough in petroleum exploration in the study area since nearly 30 years ago, until the success of KD 1 well in the FSB in 2010, which indicates significant exploration potential in the study area. However, failure of later KD 101 and KD 2 wells suggests that the hydrocarbon accumulation of this study area is complicated. This complexity should be related to the complex regional structure. The late transpressional faulting damaged early large anticline reservoir and redistributed the hydrocarbon.

The source rocks of the FSB include the Lower Carboniferous limestone, Lower Permian limestone and mudstone, and Jurassic mudstone, while they are dominated by the Lower Carboniferous and Lower Permian strata (Li et al. 1996; Mo et al. 2013; Zhang et al. 2013). Reservoir rocks in the FSB are located in several levels with the Cretaceous–Neogene sediments, such as the Cretaceous sandstone, the Paleocene Kalatar limestone and the Miocene sandstone. The Cretaceous–Neogene thick gypsum and mudstone beds constitute the main seal, trappings the hydrocarbon concentration with these series (Xing et al. 2012; He et al. 2013). Given the fertile source rocks, effective reservoir rocks, good cap rocks and migration pathway, the trap condition is the most vital factor for restricting the hydrocarbon accumulation in the FSB.

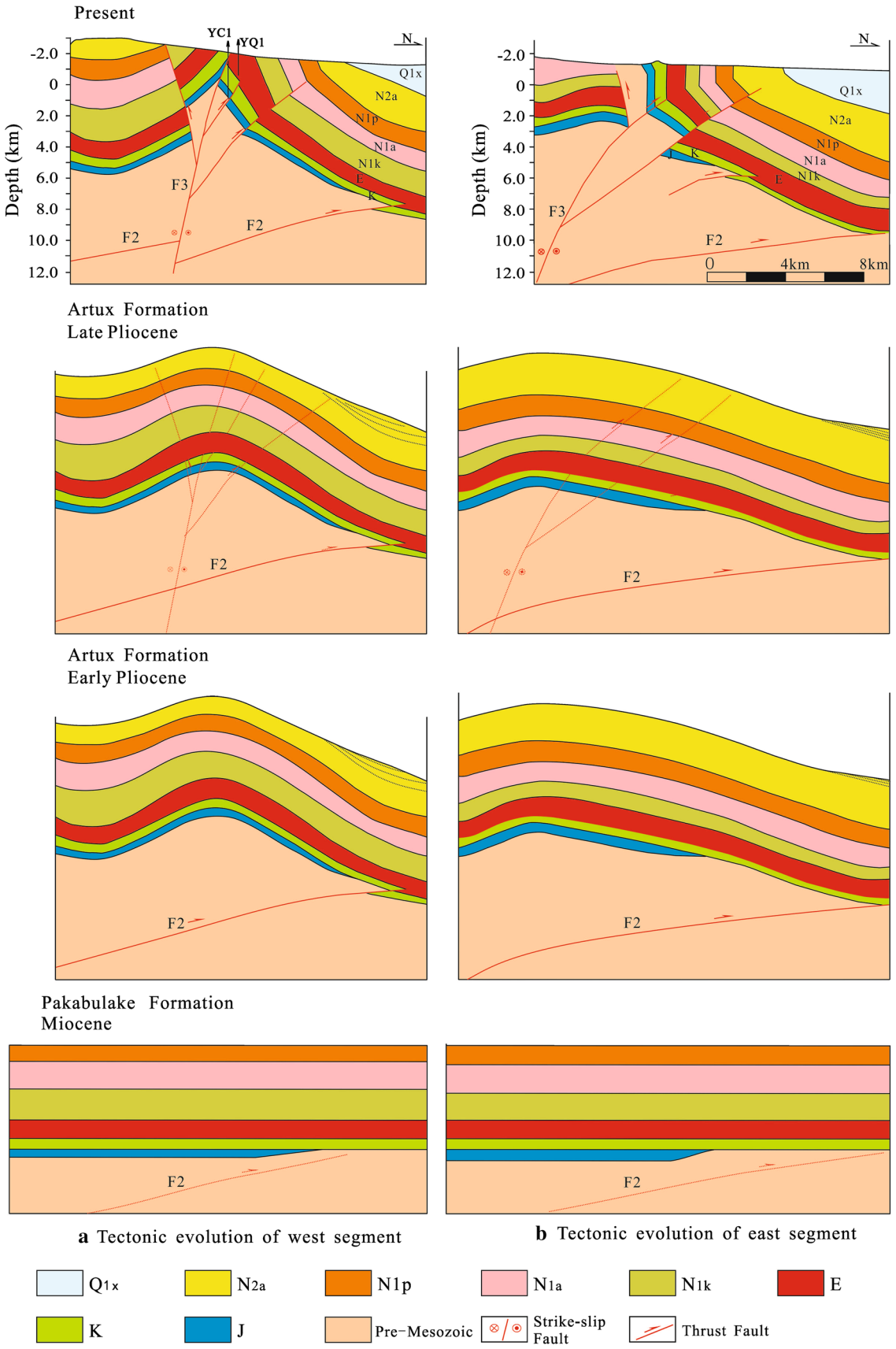


**Fig. 13** Miocene evolution of east and west segments in FSB

From Miocene to early Pliocene, the fault-propagation fold in the FSB was developed by the northward convergence of Tiklik block. Meantime, Permian source rocks situated on the stage of hydrocarbon generation, and the Carboniferous oil source rocks reached post-mature, while the Jurassic oil source rocks were still immature (Mo et al. 2013). The hydrocarbon which was from Permian oil source rocks began to fill the complete anticline. From late Pliocene to Pleistocene, the deformation of the FSB was controlled by transpressional faulting, with the steeply dipping dextral strike-slip reverse fault initiating in the middle part of the FSB and dividing the early complete anticline into several fault blocks. Moreover, this tectonic activity resulted in readjusting and distributing the oil and gas accumulation. At this time, the Permian oil source rocks reached high maturity and were dominated by generating gas. The Jurassic oil source rocks were at low mature stage and began to generate gas, while the Carboniferous oil source rocks were at the mature stage and still generated a small amount of gas. The natural gas was continually filling in the traps in this stage.

Due to the fact that the anticlines which are cut through by late strike-slip reverse fault are different between the western segment and eastern segment, the present structural types of the western segment and eastern segment are obviously different, which results in forming different traps. The late strike-slip reverse fault cuts though the core of the western anticline, and the complete anticline is divided into several fault blocks which form fault block traps. In contrast, the late strike-slip reverse fault cuts though the northern limb of eastern anticline and results in fault block traps. The anticline style is still retained in the deep in the southern area of the anticline and forms an anticlinal trap. Therefore, the western trap type is composed of fault block traps, while the eastern includes the fault block traps and anticline traps.

The migration path and fault seal ability in diverse fault blocks exert important influence on the late hydrocarbon accumulation. The strike-slip reverse fault and accompanied secondary fracture can be the good channel for oil and gas migration which destroy the primary reservoir and migrate the oil and gas, such as the KD 101 well and KD 2 well. If the fault plays a major role in sealing, the trap can restore the hydrocarbon, such as KD 1 well. Therefore, in order to search for the favorable target of oil and gas, we should focus on the stable region of early anticline and fault traps with good fault sealing.

## Conclusion

1. FSB has experienced two types of tectonic deformation since Cenozoic. The first stage was the contraction deformation, and the FSB which belongs to the Cenozoic thrust belt in front of the Western Kunlun Orogen was formed and was composed of two anticlines which were superposed near the Keliyang area in the early Pliocene. The second stage was transpressional deformation, and a steeply dipping dextral strike-slip reverse fault cuts through the anticlines, which destroyed and divided the anticline into a number of blocks since the late Pliocene.
2. The steeply dipping dextral strike-slip reverse fault presents northward convex shape in map view and varied its trend, NWW direction in the eastern segment, while EW direction in the western segment with the changing region located in the Yuliqun area. Moreover, the spatial distribution of this fault is limited, which intersects with Sanju fault to the east, and is predicted to intersect with Kusilaf fault to the west.
3. The shift from earlier contraction deformation during the early Pliocene to later transpressional deformation in the Pleistocene implies variation in regional stress field in the northwestern Tibetan Plateau at this time.
4. The trap style of the western segment is dominated by fault block trap, while the eastern segment is characterized by fault block trap and anticlinal trap. Taking into account of the target of the hydrocarbon accumulation, the relatively stable tectonic zone in the early anticline and the fault block traps with well fault sealing should be considered firstly.

**Acknowledgments** This work was funded by the National Science Foundation of China (Grant Nos. 41472181, 41330207, 41102128 and 41072154), the National S&T Major Project (Grant Nos. 2011ZX05009-001 and 2011ZX05003-002) and the Fundamental Research Funds for the Central Universities. We thank Prof. D. Jia, H.B. Li and another anonymous reviewer for comments which significantly improved the manuscript.

## References

Arnaud N, Tapponnier P, Roger F, Brunel M, Scharer U, Wen C, Xu ZQ (2003) Evidence for Mesozoic shear along the western Kunlun and Altyn-Tagh fault, northern Tibet (China). J Geophys Res Solid Earth 108(B1):2053

Bershaw J, Garzione CN, Schoenbohm L, Gehrels G, Li T (2012) Cenozoic evolution of the Pamir plateau based on stratigraphy, zircon provenance, and stable isotopes of foreland basin sediments at Oytag (Wuyitake) in the Tarim Basin (west China). J Asian Earth Sci 44:136–148

Bosboom RE, Dupont-Nivet G, Houben AJ, Brinkhuis H, Villa G, Mandic O, Stoica M, Zachariasse WJ, Guo ZJ, Li CX, Krijgsman W (2011) Late Eocene sea retreat from the Tarim Basin (west China) and concomitant Asian paleoenvironmental change. Palaeogeogr Palaeoclimatol Palaeoecol 299(3):385–398

Burtman VS (2000) Cenozoic crustal shortening between the Pamir and Tien Shan and a reconstruction of the Pamir–Tien Shan transition zone for the Cretaceous and Palaeogene. Tectonophysics 319(2):69–92

Cao K, Bernet M, Wang GC, van der Beek P, Wang A, Zhang KX, Enkelmann E (2013) Focused Pliocene–Quaternary exhumation of the Eastern Pamir domes, western China. Earth Planet Sci Lett 363:16–26

Chen J, Lu YC, Ding GY (2001) Records of late Cenozoic mountain building in western Tarim Basin: molasses, growth strata and growth unconformity. Quat Sci 21(6):528–539 **(in Chinese with English abstract)**

Chen HL, Zhang FF, Cheng XG, Liao L, Yang C (2010) The deformation features and basin-range coupling structure in the northeastern Pamir tectonic belt. Sci Geol Sin 45(1):102–112 **(in Chinese with English abstract)**

Cheng XG, Lei GL, Chen HL, Du ZL, Liao L, Luo JC, Shi J (2011) Cenozoic structural deformation of the Fusha-Keliyang area in the piedmont of the western Kunlun Mountains and its control on hydrocarbon accumulation. Acta Pet Sin 32(1):83–89 **(in Chinese with English abstract)**

Cheng XG, Chen HL, Shi J, Liao L, Du ZL, Huang ZB (2012a) Distribution characteristics and controlling factors of Jurassic–Cretaceous in the front of West Kunlun Mountains. Earth Sci 37(4):635–644 **(in Chinese with English abstract)**

Cheng XG, Huang ZB, Chen HL, Du ZL, Li K, Shi J (2012b) Fault characteristics and division of tectonic units of the thrust belt in the front of the West Kunlun Mountains. Acta Pet Sin 28(8):2591–2601 **(in Chinese with English abstract)**

Clift PD, Carter A, Krol M, Kirby E (2002) Constraints on India–Eurasia collision in the Arabian Sea region taken from the Indus Group, Ladakh Himalaya, India. Geol Soc Lond Spec Publ 195(1):97–116

Coutand I, Strecker MR, Arrowsmith JR, Hilley G, Thiede RC, Korjenkov A, Omuraliev M (2002) Late Cenozoic tectonic development of the intramontane Alai Valley (Pamir–Tien Shan region, central Asia): an example of intracontinental deformation due to the Indo-Eurasia collision. Tectonics 21(6):1–3

Cowgill E (2010) Cenozoic right-slip faulting along the eastern margin of the Pamir salient, northwestern China. Geol Soc Am Bull 122(1–2):145–161

Cowgill E, Yin A, Harrison TM, Wang XF (2003) Reconstruction of the Altyn Tagh fault based on U-Pb geochronology: role of back thrusts, mantle sutures, and heterogeneous crustal strength in forming the Tibetan Plateau. J Geophys Res Solid Earth 108(B7):2346

DeCelles PG, Robinson DM, Zandt G (2002) Implications of shortening in the Himalayan fold-thrust belt for uplift of the Tibetan Plateau. Tectonics 21(6):11–12

Dercourt J, Ricou LE, Vrielynck B (1993) Atlas Tethys palaeoenvironmental maps. Gauthier-Villars, Paris, pp 1–258

Du ZL, Liang H, Shi J, Chen C, Wang Y (2013) Cenozoic structural deformation and hydrocarbon exploration of Kedong structure in the piedmont of western Kunlun mountain. Acta Pet Sin 34(1):22–29 **(in Chinese with English abstract)**

Fang AM, Ma JY, Wang SG, Zhao Y, Hu JM (2009) Sedimentary tectonic evolution of the southwestern Tarim Basin and west Kunlun orogen since Late Paleozoic. Acta Petro Sin 25(12):3396–3406 **(in Chinese with English abstract)**

He DF, Li DS, He JY, Wu X (2013) Comparison in petroleum geology between Kuqa Depression and Southwest Depression in Tarim Basin and its exploration significance. Acta Pet Sin 34(2):201–218 **(in Chinese with English abstract)**

Hu JZ, Tan YJ, Zhang P, Zhang YQ (2008) Structural features of Cenozoic thrust-fault belts in the piedmont of southwestern Tarim basin. Earth Sci Front 15(2):222–231 **(in Chinese with English abstract)**

Jia CZ (2004) Tectonic feature and hydrocarbon of Tarim Mesozoic and Cenozoic Basin. Petroleum Industry Press, Beijing, pp 1–229 **(in Chinese)**

Jiang XD, Li ZX, Li HB (2013) Uplift of the West Kunlun Range, northern Tibetan Plateau, dominated by brittle thickening of the upper crust. Geology 41(4):439–442

Jin XC, Wang J, Chen BW, Ren LD (2003) Cenozoic depositional sequences in the piedmont of the west Kunlun and their paleogeographic and tectonic implications. J Asian Earth Sci 21(7):755–765

Li DS, Liang DG, Jia CZ, Wang G, Wu QZ, He DF (1996) Hydrocarbon accumulations in the Tarim Basin, China. AAPG Bull 80(10):1587–1603

Li DP, Zhao Y, Hu JM, Wan JL, Li XL, Zhou XK, Du SX, Pan YB, Pei JL (2007) Fission track thermochronologic constraints on plateau surface and geomorphic relief formation in the northwestern margin of the Tibetan Plateau. Acta Petrol Sin 23(5):900–910 **(in Chinese with English abstract)**

Liu S, Wang X, Wu X, Qiu B (2004) Growth strata and the deformation time of the Late Cenozoic along front belts of Pamir–western Kunlun–southwest Tianshan in China. Acta Pet Sin 25(5):24–28 **(in Chinese with English abstract)**

Liu H, Wang GC, Cao K, Yn M, Wang A, Zhang KX (2010) The detrital zircon fission-track ages constraint to tectonic processes in west Ku and adjacent regions. Earth Sci Front 17(3):64–78 **(in Chinese with English abstract)**

Matte P, Tapponnier P, Arnaud N, Bourjot L, Avouac JP, Vidal P, Liu Q, Pan YS, Wang Y (1996) Tectonics of Western Tibet, between the Tarim and the Indus. Earth Planet Sci Lett 142(3):311–330

Mo WL, Lin T, Zhang Y, Yi SW, Wang DL, Zhang L (2013) Hydrocarbon origin and accumulation model of Kedong–Kekeya tectonic belt in piedmont of West Kunlun Mountain. Pet Geol Exp 35(4):364–371 **(in Chinese with English abstract)**

Patriat P, Achache J (1984) India–Eurasia collision chronology has implications for crustal shortening and driving mechanism of plates. Nature 311(5987):615–621

Qu GS, Chen J, Chen XA, Zhang XL, Li T, Yin JP, Zhou HQ (1998) Intraplate deformation in the front of the West Kunlun-Pamir Arcuate Orogenic Belt and the Southwest Tarim Foreland Basin. Geol Rev 44(4):420–429 **(in Chinese with English abstract)**

Qu GS, Li YG, Li YF, Canerot J, Chen XF, Yin JP, Chen XA, Zhang N, Deramond J (2005) Tectonic segmentation and its origin of southwestern Tarim foreland basin. Sci China Ser D 35(3):193–202 **(in Chinese with English abstract)**

Robinson AC, Yin A, Manning CE, Harrison TM, Zhang SH, Wang XF (2004) Tectonic evolution of the northeastern Pamir: constraints from the northern portion of the Cenozoic Kongur Shan extensional system, western China. Geol Soc Am Bull 116(7–8):953–973

Robinson AC, Yin A, Manning CE, Harrison TM, Zhang S, Wang XF (2007) Cenozoic evolution of the eastern Pamir: implications for strain-accommodation mechanisms at the western end of the Himalayan–Tibetan orogen. Geol Soc Am Bull 119(7–8):882–896

Robinson AC, Ducea M, Lapen TJ (2012) Detrital zircon and isotopic constraints on the crustal architecture and tectonic evolution of the northeastern Pamir. Tectonics 31(2):TC2016

Searle MP, Windley BF, Coward MP, Cooper DJW, Rex D, Li TD, Xiao XC, Jan MQ (1987) The closing of Tethys and the tectonics of the Himalaya. Geol Soc Am Bull 98(6):678–701

Si JL, Li HB, Laurie B, Jerome VDW, Sun ZM, Pei JL, Pan JW (2007) Late Cenozoic uplift of the northwestern margin of the Qinghai–Tibet Plateau: sedimentary evidence from piedmont basins of the West Kunlun Mountains. Geol Bull China 26(10):1356–1367 **(in Chinese with English abstract)**

Sobel ER (1999) Basin analysis of the Jurassic–Lower Cretaceous southwest Tarim basin, northwest China. Geol Soc Am Bull 111(5):709–724

Sobel ER, Dumitru TA (1997) Thrusting and exhumation around the margins of the western Tarim basin during the India-Asia collision. J Geophys Res Solid Earth 102(B3):5043–5063

Sun JM, Jiang MS (2013) Eocene seawater retreat from the southwest Tarim Basin and implications for early Cenozoic tectonic evolution in the Pamir Plateau. Tectonophysics 588:27–38

Sun JM, Liu DS (2006) The age of the Taklimakan Desert. Science 312(5780):1621

Suppe J, Chou GT, Hook SC (1992) Rates of folding and faulting determined from growth strata. In: McClay KR (ed) Thrust tectonics. Chapman & Hall, London, pp 105–121

Tapponnier P, Peltzer G, Armijo R (1986) On the mechanics of the collision between India and Asia. Geol Soc Lond Spec Publ 19(1):113–157

Wan JL, Wang E (2002) FT evidence of west Kunlun uplift in Pulu. Nucl Tech 25(7):565–567 **(in Chinese with English abstract)**

Wang E, Wan JL, Liu JQ (2003) Late Cenozoic geological evolution of the foreland basin bordering the West Kunlun range in Pulu area: constraints on timing of uplift of northern margin of the Tibetan Plateau. J Geophys Res Solid Earth 108(B8):2401

Wang X, Sun DH, Chen FH, Wang F, Li BF, Popov SV, Wu S, Zhang YB, Li ZJ (2014) Cenozoic paleo-environmental evolution of the Pamir–Tien Shan convergence zone. J Asian Earth Sci 80:84–100

Wu XF, Liu S, Wang X, Yang SF, Gu X (2004) Analysis on structural sections in the Cenozoic Pamir–Western Kunlun foreland fold-and-thrust belt. Scientia Geologica Sinica 39(2):260–271 **(in Chinese with English abstract)**

Xiang K (2006) Transpressional structural systems and their petroleum geological significance in southwestern margin of Tarim Basin. J Palaeogeogr 8(2):233–240 **(in Chinese with English abstract)**

Xiao AC, Yang SF, Chen HL, Jia CZ, Wei GQ (2000) Structural characteristics of thrust system in the front of the West Kunlun Mountains. Earth Sci Front 7(Supplement):38–43 **(in Chinese with English abstract)**

Xing HS, Li J, Sun HY, Wang H, Yang Q, Shao LY, Yang D, Yang S (2012) Differences of hydrocarbon reservoir forming between Southwestern Tarim Basin and Kuche Mountain Front. Nat Gas Geosci 23(1):36–45 **(in Chinese with English abstract)**

Yang HJ, Wang BQ, Yang ZL, Lei GL, Wei HX (2011) Structure modeling and hydrocarbon exploration of Kedong structural belt in southwestern Tarim Basin. Dizhi Kexue/Chin J Geol 46(2):456–465 **(in Chinese with English abstract)**

Yin A, Rumelhart PE, Butler R, Cowgill E, Harrison TM, Foster DA, Ingersoll RV, Zhang Q, Zhou XQ, Wang XF, Hanson A, Raza A (2002) Tectonic history of the Altyn Tagh fault system in northern Tibet inferred from Cenozoic sedimentation. Geol Soc Am Bull 114(10):1257–1295

Zeng CM, Du ZL, Zhou XH, Feng XJ, Guo QY, Wei W (2011) Structural characteristics and deformation mechanism of Kedong Thrust Belt in Piedmont of Kunlun Mountain. Xinjiang Pet Geol 32(2):133–136 **(in Chinese with English abstract)**

Zhang CS, Xiao AC, Li JY, Shi D (2000) Depositional feature of Jurassic Fault Basin in southwest Tarim depression. J Mineral Petrol 20(3):41–45 **(in Chinese with English abstract)**

Zhang SB, Ni YN, Gong FH, Lu HN, Huang ZB, Lin HL (2003) A guide to the stratigraphic investigation on the peripheral of the Tarim Basin. Petroleum Industry Press, Beijing, pp 1–280 **(in Chinese)**

Zhang W, Qi JF, Li Y (2011) Structural styles in South-western margin of Tarim Basin and their dominate factors. Chin J Geol 46(3):723–732 **(in Chinese with English abstract)**

Zhang L, Zeng CM, Huang ZB, Chen C, Zhu LC, Shen CG, Lv HX (2013) The characteristics of crude oil from Cretaceous in No. 1 Kedong Structure of Southwest Depression in the Tarim Basin. Xinjiang. Geology 31(2):199–201 **(in Chinese with English abstract)**

Zheng HB, Powell CM, An ZS, Zhou J, Dong GR (2000) Pliocene uplift of the northern Tibetan Plateau. Geology 28(8):715–718

Zheng HB, Butcher K, Powell CM (2002) Evolution of Neogene foreland basin in Yecheng, Xinjiang, and uplift of northern Tibetan plateau-I stratigraphy and petrology. Acta Sedimentol Sin 20(2):274–281 **(in Chinese with English abstract)**

Zheng HB, Butcher K, Powell CM (2003a) Evolution of Neogene foreland basin in Yecheng, Xinjiang, and uplift of Northern Tibetan Plateau-II Facies analysis. Acta Sedimentol Sin 21(1):46–51 **(in Chinese with English abstract)**

Zheng HB, Powell CM, Butcher K, Cao JJ (2003b) Late Neogene loess deposition in southern Tarim Basin: tectonic and palaeoenvironmental implications. Tectonophysics 375(1):49–59

Zheng HB, Huang XT, Butcher K (2006) Lithostratigraphy, petrography and facies analysis of the Late Cenozoic sediments in the foreland basin of the West Kunlun. Palaeogeogr Palaeoclimatol Palaeoecol 241(1):61–78